Published in final edited form as:
Nat Photonics. 2013 May ; 7(5): 400–406. doi:10.1038/nphoton.2013.34.

A polymer optoelectronic interface restores light sensitivity in blind rat retinas

Diego Ghezzi[1], **Maria Rosa Antognazza**[2], **Rita Maccarone**[3], **Sebastiano Bellani**[2], **Erica Lanzarini**[2], **Nicola Martino**[2], **Maurizio Mete**[4], **Grazia Pertile**[4], **Silvia Bisti**[3], **Guglielmo Lanzani**[2,*], and **Fabio Benfenati**[1,5,*]

[1]Department of Neuroscience and Brain Technologies, Istituto Italiano di Tecnologia, Genova, Italy

[2]Center for Nano Science and Technology@PoliMi, Istituto Italiano di Tecnologia, Milano, Italy

[3]Dipartimento di Tecnologie Biomediche, Università dell'Aquila, L'Aquila, Italy

[4]UO Oculistica, Ospedale S. Cuore-Don Calabria, Negrar, Italy

[5]Department of Experimental Medicine, University of Genova, Genova, Italy

Abstract

Interfacing organic electronics with biological substrates offers new possibilities for biotechnology due to the beneficial properties exhibited by organic conducting polymers. These polymers have been used for cellular interfaces in several fashions, including cellular scaffolds, neural probes, biosensors and actuators for drug release. Recently, an organic photovoltaic blend has been exploited for neuronal stimulation via a photo-excitation process. Here, we document the use of a single-component organic film of poly(3-hexylthiophene) (P3HT) to trigger neuronal firing upon illumination. Moreover, we demonstrate that this bio-organic interface restored light sensitivity in explants of rat retinas with light-induced photoreceptor degeneration. These findings suggest that all-organic devices may play an important future role in sub-retinal prosthetic implants.

Extracellular electrical stimulation of neurons represents the foundation of many implantable prosthetic devices, which help to restore motor activity (such as electrodes for functional electrical stimulation[1,2]), treat drug-resistant Parkinson's disease (such as implants for deep brain stimulation[3] and restore sensory perception (such as cochlear

*Correspondence and requests for materials should be addressed to G.L. and F.B. fabio.benfenati@iit.it and guglielmo.lanzani@iit.it.

Author contributions D.G. prepared cell cultures, degenerate animals and retinal explants, planned experiments, performed photo-stimulation experiments and cell viability assay, analysed data and wrote the manuscript. M.R.A planned experiments, discussed results and wrote the manuscript. R.M. prepared degenerate animals, performed retinal sections and acquired confocal images. E.L. prepared polymer samples. Se.Be., E.L. and N.M. performed polymer film electro-optical characterization and analysed data. M.M. and G.P. discussed results. Si.Bi. discussed electrophysiological experiments with retinal explants. G.L. and F.B. planned experiments, interpreted and discussed the data, wrote the manuscript and supported the research. All the authors discussed the results and revised the manuscript.

Additional information Supplementary information is available in the online version of the paper. Reprints and permission information is available online at http://www.nature.com/reprints.

Competing Financial interests The authors declare no competing financial interests.

Europe PMC Funders Author Manuscripts

implants[4] or retinal prosthesis[5-7]. In the last decade, much effort has been dedicated to improving the interfaces between electrodes and neuronal tissues. Many issues related to biological affinity, biocompatibility, mechanical flexibility, ease of functionalisation and cost effectiveness have been extensively investigated. Conversely, the use of light-enabled processes for cell stimulation has received much less attention, with the exception of the outstanding progress made in optogenetic techniques in the last few years[8,9]. Given this scenario, the interfacing of organic electronics and biological substrates offers new possibilities[10-12]. Organic conducting polymers have been widely employed as culturing substrates[13], 3D scaffolds[14], electrode coatings[15,16], organic biosensors[17,18], actuators for drug release[19,20] and organic electrodes for controlling cell seeding[21], growth[22,23] and activity detection[24]. Recently, an organic photovoltaic device has also been exploited for neuronal photo-stimulation[25,26]. This system provides interesting improvements as compared to inorganic semiconductors[5,27,28] and has great potential for *in-vivo* biological applications, such as retinal prostheses.

In photovoltaic applications, the electron donor-acceptor mechanism is currently the basis of the most efficient organic solar cells. This mechanism takes advantage of the bulk heterojunction architecture to widen the interface between donor and acceptor, maximise the probability of charge pair separation and limit the charge recombination process. Accordingly, one of the most successful photovoltaic blends, namely a mixture of *poly(3-hexylthiophene)* and *phenyl-C_{61}-butyric-acid-methyl ester* (P3HT:PCBM), has proven to be effective in directly photo-stimulating neurons grown at the interface[25,26]. However, once in contact with the biological environment, such bio-hybrid devices may have functional mechanisms that differ from those of conventional solar cells in which the extraction of photo-generated electrical charges is usually achieved by the aforementioned bulk heterojunction geometry. Conversely, the neuronal photo-stimulation process is most likely mediated via capacitive charging of the polymer-electrolyte interface rather than an electron transfer phenomenon. In addition, fullerenes have been demonstrated to produce reactive oxygen species upon illumination[29]. Based on these considerations, we hypothesised that the electron donor-acceptor interface may not represent the best possible strategy to drive neuronal activity. In this work, we demonstrate that a simpler active layer, constituted by the only donor component (P3HT), can efficiently stimulate primary neurons upon illumination and restore light sensitivity in explanted degenerate retinas.

Interface characterisation

We first investigated whether illumination of a pure P3HT film is able to locally modify the electric equilibrium at the polymer/electrolyte interface and thus generate a stimulus that is able to induce membrane depolarisation in neurons. To this aim, we evaluated the temporal and spatial properties of the photocurrent elicited by a pulsed illumination with a patch pipette in voltage-clamp mode that was positioned in close proximity (< 5 μm) to the P3HT layer (Fig. 1a). A pulsed illumination (20 ms, 15 mW/mm^2) of the polymer area under the electrode generated large (142.6 ± 7.4 pA, n = 12, mean ± s.e.m.) and fast (43.4 ± 2.2 pA/ms, n = 12, mean ± s.e.m.) ionic currents (Fig. 1b). The sign of the current was consistent with the generation of an excess negative charge underneath the electrode, while the rest of the electrolyte (including the reference electrode) remained relatively positive.

Moreover, by illuminating the P3HT surface with repetitive pulses (20 ms, 15 mW/mm^2) at a frequency of 2 Hz (Fig. 1c), the photo-current generated during the train decayed very slowly (last response: 72.83 ± 0.86 % of the first response), thereby potentially allowing the application of train pulses for repetitive neuronal stimulation.

To understand the gradient distribution of the photo-generated current, we examined the intensity profile of the photo-current by progressively increasing the pipette distance from the illuminated spot in the horizontal and vertical planes (Fig. 1d). Outside of the light spot (distances greater than 50 μm from the centre), the intensity of the photo-current was dramatically reduced (42 % reduction at 25 μm from the spot edge) with an exponential profile (Fig. 1e). Similarly, we observed an exponential decrease of the photo-generated current with increasing distance from the polymer-electrolyte interface (Fig. 1f). These observations confirm that the charge accumulation in response to illumination occurs at the polymer/electrolyte interface and is localised to the illuminated area.

Photo-stimulation of primary neurons

We then asked whether the P3HT photovoltaic layer was able to excite primary neurons cultured on the polymer surface through the generation of local stimuli in the electrolyte upon illumination. Rat hippocampal neurons were grown onto P3HT-coated Glass:ITO substrates and analysed at 18-21 days *in-vitro* (DIV) with viability assays and patch-clamp recordings (Fig. 2a). Biocompatibility of the P3HT-PCBM blend has previously been demonstrated in cultured hippocampal neurons[26]. As an additional control, we performed a cell viability assay (Supplementary Fig. 1a) of neurons cultured on either P3HT-coated Glass:ITO or control Glass:ITO substrates at 21 DIV. No significant differences were found in either cell viability (Supplementary Fig. 1b, Student's *t*-test, P = 0.818, $n = 6$) or mortality (Supplementary Fig. 1c, Student's *t*-test, P = 0.639, $n = 6$) under these culture conditions, indicating that the P3HT layer did not alter neuronal viability over a long period of time. As further proof of cell viability, comparison of the resting membrane potential of neurons cultured on either P3HT-coated Glass:ITO or control Glass:ITO substrates did not reveal any significant difference (Supplementary Fig. 1d, Student's *t*-test, P = 0.128).

When neuronal activity was assessed by patch-clamp analysis in current-clamp configuration, we found that a light pulse (20 ms, 15 mW/mm^2) was able to depolarise neurons and induce them to fire action potentials (Fig. 2b, left panel) with short peak latencies and a negligible latency jitter (Fig. 2b, right panel). The latter parameters were in the same order of magnitude as those previously reported[26] for the P3HT-PCBM blend (Peak latency: P3HT 11.21 ± 0.21, P3HT-PCBM 11.32 ± 0.17 ms, P = 0.746, means ± s.e.m., Student's *t*-test; latency jitter: P3HT 0.98 ± 0.12, P3HT-PCBM 1.48 ± 0.25 ms, P = 0.361; means ± s.e.m., Student's *t*-test). In contrast, light stimulation was virtually ineffective for neurons grown onto control Glass:ITO coverslips (Fig. 2b, left panel). Moreover, we were able to effectively trigger spike trains at up to 20 Hz of pulsed illumination with high reproducibility in the 1-10 Hz range (Fig. 2c) and a limited number of failures that was only present at 20 Hz (inset of Fig. 2c). The percentage of successful spikes in the train, computed over all recorded neurons as a function of the stimulation frequency, confirmed the tight coupling between light stimulation and firing frequencies (Fig. 2d). The

optimal pulse duration was chosen by testing various pulse widths with a train stimulation of 20 pulses delivered at 1 Hz (Supplementary Fig. 2a). Using a pulse of 20 ms, the number of successful spikes in a train of 20 pulses was approximately 100 % (96.67 ± 1.67 %, mean ± s.e.m.; Supplementary Fig. 2b). Under this condition, the depolarising current amplitude measured by patch-clamp analysis in voltage-clamp configuration at a holding potential of −60 mV was −75.51 ± 4.61 pA (mean ± s.e.m., $n = 5$).

To evaluate the efficiency of the single donor component active layer in depolarising neurons, we compared the extent of neuronal depolarisation to that obtained with the P3HT-PCBM blend active layer by performing current-clamp experiments in the presence of tetrodotoxin (TTX, 1 μM), a blocker of voltage-dependent Na^+ channels that inhibits action potential generation (Supplementary Fig. 3a). The amplitudes of depolarisation elicited by light pulses of various durations (20-100 ms) were similar regardless of the presence of PCBM in the active layer (Supplementary Fig. 3b). Moreover, no detectable differences in the resting potentials were observed in neurons cultured onto either Glass:ITO, P3HT-coated Glass:ITO or P3HT:PCBM-coated Glass:ITO substrates in the presence of TTX (Supplementary Fig. 3c).

Photo-stimulation of retinal explants

The high spatial and temporal resolution demonstrated by the P3HT active layer in stimulating cultured neurons, together with the properties of the polymer interface (biocompatibility, no external bias or heat generation), suggests a potential application in the field of retinal prostheses. Thus, we investigated the ability of the polymer layer to restore light sensitivity in retinas explanted from albino rats with a light-induced degeneration of the photoreceptor layer (Fig. 3a,b). Acutely dissected retinas were placed on either P3HT-coated Glass:ITO or Glass:ITO alone in a sub-retinal configuration (i.e., external layers in contact with the polymer). As an additional control, retinas from littermates housed under dim light conditions were also analysed. Multi-unit activity (MUA) recordings, performed with an extracellular electrode in the retinal ganglion cell (RGC) layer and representing the output response of the retina to light, showed that a light stimulus (10 ms, 4 mW/mm^2; 16-fold lower than the safe limit for pulsed illumination that can be delivered to the retina in ophthalmic application, see Methods) failed to induce spiking activity in degenerate retinas on Glass:ITO, while this stimulus elicited intense activity in control retinas. Strikingly, light-induced spiking activity was rescued in degenerate retinas placed on P3HT-coated Glass:ITO to levels indistinguishable from those recorded in control retinas (Fig. 4a,b). The latter response appeared with a delay of approximately 70-100 ms after the onset of the light pulse and was specifically blocked by TTX (Supplementary Fig. 4). The response latency and the persistence of the local field potential (LFP) associated with the synaptic activity indicated that the firing of RGCs in degenerate retinas was mediated by the activation of the external cell layers interfaced with the polymer. To evaluate the efficiency of the retinal interface, dose-response analyses of both spiking activity (Fig. 4c) and LFP amplitude (Supplementary Fig. 5) *versus* light intensity were performed in degenerate retinas recorded over P3HT-coated Glass:ITO or Glass:ITO alone. Remarkably, spiking activity was observed in degenerate retinas over the polymer with a response threshold (10 % of maximal amplitude) below 0.3 $\mu W/mm^2$, a linear increase in the 1-100 $\mu W/mm^2$ range and a response saturation

(90% of maximal amplitude) at 100 μW/mm^2 (still below the safe limit of radiant power that can be delivered chronically to the retina in ophthalmic applications, see Methods). In contrast, spiking activity in degenerate retinas recorded over Glass:ITO displayed low levels of spiking activity only at very high light intensity (threshold**,** 80 μW/mm^2; Fig. 4c). A 4-fold increase in the amplitude of the light response at saturation and a significant left shift of the dose-response curves were obtained in retinas placed over the P3HT-coated interface. Consistent results (threshold for the response below 0.2 μW/mm^2; linear response in the 1-100 μW/mm^2 range; response saturation at 100 μW/mm^2) were also observed in the dose-response analysis of LFP amplitudes (Supplementary Fig. 5).

Discussion

We documented that a single component organic polymer film is sufficient to build efficient opto-neuronal interfaces. We investigated this novel polymer-electrolyte system by measuring the photo-current locally generated at the interface, characterising the effect of the biological environment on the properties of the polymer film and identifying the mechanisms leading to efficient neuronal photo-excitation. The use of the single P3HT component seems particularly favourable for reducing material toxicity during light exposure, as fullerene photo-excitation has been reported to result in singlet oxygen formation from the triplet state[29].

We demonstrate that, although poorly efficient as a solar cell, once the P3HT film is in contact with an electrolytic solution, it becomes capable of depolarising neurons upon illumination with high reproducibility in a manner similar to that previously observed with bulk heterojunction (P3HT-PCBM blend)[26]. These findings indicate that the two configurations are equivalent for the purpose of interfacing organic polymers with biological tissues. This is consistent with an effective charge dissociation occurring mainly at the interface with ITO, with minor contributions of carriers generated in the bulk (where the presence of PCBM is crucial for efficient dissociation). We also found that contact with the electrolyte was associated with an increase in *p*-doping of P3HT polymer, a process likely mediated by molecular oxygen that causes oxidation of the polymer and the generation of free holes (see Supplementary Results and Supplementary Fig. 6). The analysis of the photo-current resulting from the interface polarisation was compatible with an accumulation of negative charges at the illuminated polymer surface that attract positive ions from the electrolytic solution and from the liquid shell wetting the external face of the neuronal membrane. Thus, stripping the excess extracellular positive charge is the likely mechanism that triggers membrane depolarisation and, eventually, neuronal firing.

The ability of the organic interface to photo-stimulate neurons prompted us to investigate its efficacy in restoring light sensitivity to blind retinas. Sight restoration in blind people is one of the new frontiers for prosthetic devices that enable the electrical stimulation of neurons. In particular, diseases that affect the retinal pigment epithelium and photoreceptors but preserve the inner retinal layers, such as *Retinitis pigmentosa*, Stargardt's disease or age-related macular degeneration, are preferential targets for implantation of visual prostheses. Several approaches for the treatment of patients with degenerative diseases of the outer retina have previously been described[30], including the regeneration of lost photoreceptors by

means of transplantation[31,32], gene therapy[33] or the use of artificial/engineered photoreceptors. The last category includes the implant of retinal prosthetic devices or the expression of microbial opsins[34,35]. Optogenetic probes are an emerging, widely used tool in neuroscience, but their application in humans remains limited by the viral expression of the probes. In contrast, silicon-based retinal prosthetic devices implanted in either epi-retinal or sub-retinal[6,7] configuration have entered the level of clinical experimentation and yielded partial sight restoration. However, no retinal prosthesis reported thus far is totally autonomous in functioning; existing silicon-based electronic devices remain limited by the electrode spatial resolution and the requirement for connections in data processing and/or a power supply. Recently, an elegant solution based on silicon photodiodes driven by a near-infrared illumination was proposed to eliminate the need for cables[5]. However, this solution still requires the use of a goggle-embedded imaging-capturing camera[36] that can potentially cause image fading during head/eye movements. Finally, it has recently been reported that the intraocular injection of a photo-switchable probe transiently restores light sensitivity in mouse models of *Retinitis pigmentosa* without any exogenous gene delivery[37].

The possibility of photo-stimulating neurons via an organic interface prompted us to test the efficacy of this method in retinas explanted from albino rats with reproducibly induced photoreceptor degeneration due to light damage[38,39]. However, while primary neurons grow strictly in adhesion with the polymer surface, we dealt with the possibility that the interface coupling with an intact tissue such as the retina explant would be less effective and potentially associated with higher impedance values. Despite these concerns, the mono-component interface in the sub-retinal configuration was extremely efficient in eliciting local field potentials in the retinal networks and action potential firing of the RGCs to levels indistinguishable from normal retinas (Fig. 4b). This finding indicates that the interface is able to substitute photoreceptors in activating the processing of the inner retina and to rescue light sensitivity.

Natural rod photoreceptors have an inherent amplification system for increasing light sensitivity, which is represented by stacks of disks rich in the light-sensitive molecule rhodopsin. Light sensitivity is therefore an incredible challenge for the generation of retinal prostheses. Many proposed approaches are not sensitive enough to irradiance levels in the daylight range and require external light projectors, whose design should take into account the maximum permissible exposures for ocular safety allowed for ophthalmic applications[40]. Interestingly, our organic photovoltaic device proved to possess a remarkable light-sensitivity, with a response threshold of 0.3 μW/mm^2, 30-fold lower than the ocular safety limit for continuous exposure to visible light (106.93 μW/mm^2), and a response saturation at 100 μW/mm^2, still below the limit. Moreover, the response threshold closely matched the range (0.1-10 μW/mm^2) of retinal irradiance during common daily outdoor activity[41,42], thus suggesting a possible future implementation without any external light projectors. Another interesting feature of our interface is related to the linear dynamic range of operation covering 2 log units of retinal irradiation (1-100 μW/mm^2). This linear operating range allows the modulation of the retinal output (ganglion cell spiking activity) depending on the light dose reaching the polymer/retina interface. As a result, the peak spiking activity of ganglion cells could be tuned between 1 and 30 Hz (Fig. 4c, right panel). The possibility to directly modulate the retinal spiking output depending on the light dose is an extremely

important requirement in developing artificial prosthesis aimed at restoring the physiological function of the retina.

Notwithstanding these promising results, some improvements on the light sensitivity and on the gain of the linear range are still needed to match the physiological functioning of the retina. The documented linear dynamic range of the organic device (1-100 μW/mm^2) only partially covers the range (0.1-10 μW/mm^2) of daylight retinal irradiance, thus requiring an increase in light sensitivity or in the stimulation efficiency. Moreover, the linear gain in the output spiking (1 to 30 Hz in 2 log units of retinal irradiation) is lower than the typical gain of spiking activity of RGCs under physiological conditions. Several possible strategies can be envisaged to improve the organic bio-interface performances, such as: (i) a fine tuning of the active layer film thickness and the use of a higher mobility semiconducting polymer to enhance the number of absorbed photons and thus the number of charge carriers, (ii) multilayer architecture of the device to broaden the spectral sensitivity and (iii) improvement of the wettability of the polymer surface through proper chemical engineering and/or realization of 3D micro-structured polymer scaffold to lower the impedance of the electrical contact. The combination of the mentioned and other possible strategies will help in developing a new generation of fully organic prosthetic devices for sub-retinal implants.

In addition to this indispensable feature, the organic photovoltaic interface has many potential advantages over previously proposed devices for *in-vivo* applications, including biocompatibility, freedom from the need of external bias or power supply, negligible heat generation, absorption in the green-orange region of the visible spectrum (closely resembling the spectral sensitivity of rods and M-cones) and high spatial and temporal resolution in response to pulsed illumination. As far as spatial resolution is concerned, we previously showed that the uncoupling between the light stimulus and neuronal firing occurs at a distance between the light stimulus and the centre of the neuronal soma greater than 20 μm[26]. This value can be considered as a superior limit for the spatial resolution of our device and is confirmed by the observation that the photo-current strongly decreases after such distance (42 % reduction at 25 μm from the spot edge, Fig. 1e). Although this value is not comparable with the spatial resolution and integration properties of the retinal cones, the possibility to obtain localized stimulation (at least in a range of 20 μm) with a continuous active layer represents a distinct advantage respect to electrode-based devices with inherent fixed geometry.

In conclusion, our findings demonstrate that a P3HT pristine polymer film is able to trigger photo-stimulation of primary neurons, acts as an artificial photoreceptor layer and restores light sensitivity in explanted retinas from animal models of photoreceptor degeneration. Although the dynamic range of the polymeric film is not yet comparable to the wide range of luminances that rods and cones can handle, these finding broaden the possibility of developing a new generation of fully organic prosthetic devices for sub-retinal implants with sensitivity to irradiances compatible with physiological levels of illumination.

Methods

Preparation of the organic conducting polymers

rr-P3HT (Sigma-Aldrich) has a regio-regularity of 99.5 % and a molecular weight of 17,500 g/mol; it was used without any further purification. As thorough cleaning of the substrate was required, rinses were performed in an ultrasonic bath with the following sequential solutions: a specific tension-active agent in a water solution (HELLMANEX® II, 3 %), deionised water, pure acetone and isopropyl alcohol. Oxygen plasma cleaning of the substrate completed the process. 1,2-Dichlorobenzene solutions of P3HT and PCBM were prepared separately. P3HT was diluted to a concentration of 30 g/l when used as a single active layer. PCBM was prepared at a concentration of 30 g/l and then mixed (1:1 volume ratio) with P3HT (30 g/l) using a magnetic stirrer. Solutions were then heated to 50 °C for 20 min, stirred and finally deposited onto previously heated ITO-covered squared glass substrates (18 mm side, 180 μm thickness, 10 Ω/sq resistance; Nanocs) by spin-coating. The spinning parameters (P3HT: first step 800 rpm, angular acceleration 1,500 rad/s, rotation duration 30 s; second step 1,500 rpm, angular acceleration 4,000 rad/s, rotation duration 30 s; P3HT:PCBM: first step 800 rpm, angular acceleration 1,500 rad/s, rotation duration 2 s; second step 1,500 rpm, angular acceleration 4,000 rad/s, rotation duration 30 s) were carefully selected to obtain suitable optical quality and film thickness (P3HT: 230 nm; P3HT:PCBM: 170 nm). After deposition, organic layers were annealed and properly sterilised by heating to 120 °C for 2 hr. ITO-coated glass substrates were properly sterilised in the same way.

Photoreceptor degeneration and explants

As previously described[38] Sprague-Dawley albino rats were reared in cages containing two animals, fed ad libitum, and kept on a 12 hr:12 hr light-dark cycle (light intensity between 5 and 10 lx) from birth. To induce photoreceptor degeneration, 2-month-old animals were exposed to bright (1.000 lx) light generated by a white fluorescent source for 72 hr after an overnight dark adaptation. Animals were then returned to the 12 hr:12 hr light-dark cycle. Untreated animals were maintained on a 12 hr:12 hr light-dark cycle (light intensity between 5 and 10 lx). Four to six weeks after light damage, animals were dark-adapted for at least 2 hr and anesthetised with isofluorane. The dissection procedure was performed in the dark under infrared illumination with only occasional exposure to dim red light. Eyes were enucleated and transferred to a Petri dish containing carboxygenated Ames medium (Sigma-Aldrich). The cornea, iris, lens, and vitreous were subsequently removed, and the retina was detached from the sclera. The dorsal part of each retina was sub-divided into two pieces that were placed, photoreceptor side down, over either the Glass:ITO or the P3HT-coated Glass:ITO substrate. Samples were finally transferred to the microscope stage, where they were continuously perfused with carboxygenated Ames medium heated to 35 °C. All animal manipulations and procedures were performed in accordance with the guidelines established by the European Community Council (Directive 2012/63/EU of September 22nd, 2010) and were approved by the Italian Ministry of Health.

Photo-stimulation

Light stimulation was performed on a set-up consisting of a Nikon FN1 upright microscope (Nikon Instruments). Photo-stimulation was obtained using a wide-band, high-power LED (peak at 532 nm, OPTOLED, Cairn Research). A circular illumination spot (diameter of approximately 100 μm) around the neuron was obtained by passing light through a pin hole and focusing the light with a 16x/0.8 NA water immersion objective (Nikon Instruments).

Electrophysiology

Whole-cell patch-clamp recordings of cultured neurons were performed at room temperature using patch pipettes (4-6 MΩ), under GΩ patch seals with an Axopatch 200B (Axon Instruments). The recording extracellular solution contained the following (mM): NaCl (135), KCl (5.4), $MgCl_2$ (1), $CaCl_2$ (1.8), HEPES (5), glucose (10) and pH 7.4 adjusted with NaOH. The intracellular solution contained the following (mM): K-gluconate (126), KCl (4), $MgSO_4$ (1), $CaCl_2$ (0.02), BAPTA (0.1), Glucose (15), HEPES (5), ATP (3), GTP (0.1), and pH 7.3 adjusted with KOH. Responses were amplified, low-pass filtered at 10 kHz, digitised at 50 kHz, stored and analysed with pCLAMP 10 (Axon Instruments). *Multi-Unit Recordings* of acute retinal explants were performed with glass pipettes (2-3 MΩ) filled with Ames medium, amplified and band-pass filtered at 0.1-3,000 Hz using a DAM80 amplifier (World Precision Instruments), digitised at 20 kHz, stored and analysed with pCLAMP 10. Data for spike detection were band-pass filtered at 100-3,000 Hz, and LFP data were band-pass filtered at 0.1-300 Hz. *Photo-current measurements* were performed at room temperature in recording extracellular solution with patch-pipettes (4-6 MΩ) filled with the same solution using the Axopatch 200B amplifier in voltage-clamp mode. Responses were amplified, low-pass filtered at 1 kHz, digitised at 20 kHz, stored and analysed with pCLAMP 10.

Optical safety considerations

According to ocular safety standards for ophthalmic applications[40], we calculated the maximum permissible radiant power (MPΦ) that could enter the pupil chronically or in a single short exposure. *For single-pulse exposures* (between 50 μs and 70 ms) at 532 nm, the peak limit was described by the equation $MP\Phi = 6.93 \times 10^{-4}\ C_T C_E\ t^{-0.25} = 146.17$ mW, where t = 0.01 s, $C_T = 1$ in the range of 400-700 nm and C_E is a function of the visual angle α; for retinal spot sizes greater than 1.7 mm, $\alpha = \alpha_{max} = 100$ mrad and $C_E = 6.67 \times 10^{-3}\ \alpha^2 = 66.7$ W. *For chronic exposures,* the maximum permissible radiant power was the more conservative of the thermal and photoacoustic MPΦ and the photochemical MPΦ. For thermal and photoacoustic damage, $MP\Phi = 6.93 \times 10^{-5}\ C_T C_E\ P^{-1} = 849.69$ μW, where $C_T = 1$, P = 5.44 and $C_E = 66.7$ W. For photochemical damage, $MP\Phi = 5.56 \times 10^{-10}\ C_B\ \alpha^2 = 242.70$ mW, where $C_B = 10^{0.02(\lambda-450)} = 43.65$ at 532 nm and α is the visual angle (for long exposures, α was set to $\alpha_{max} = 100$ mrad). Thus, for chronic exposures, MPΦ = 242.70 μW. In Maxwellian illumination, which is often used in ophthalmic instruments, the maximum permissible retinal radiant exposure MPH_r is given by the power entering the pupil Φ divided by the retinal exposed area. For $\alpha = \alpha_{max} = 100$ mrad the dimension of the exposed retina is assumed to be 1.7 mm in diameter. Thus for single-pulse exposure $MPH_r = 64.40$ mW/mm^2 and for chronic exposure $MPH_r = 106.93$ μW/mm^2.

Europe PMC Funders Author Manuscripts

Supplementary Material

Refer to Web version on PubMed Central for supplementary material.

Acknowledgements

The authors thank Marina Nanni, Giacomo Pruzzo and Francesa Succol for technical advice and Marco dal Maschio and Pietro Baldelli for help in data interpretation and useful discussions. We also thank Alan J. Heeger, Paul Greengard, Leo M. Chalupa and Lamberto Maffei for critical reading of the manuscript. The research was supported by the FP7-PEOPLE-212-ITN ("OLIMPIA" grant #316832), the Fondazione Istituto Italiano di Tecnologia ("Multidisciplinary Projects" call) and Telethon – Italy (GGP12033 grant to GL, FB and SB). The support by Marzio Monti and by Rolando and Ilaria Munari Gloder is also greatly acknowledged. The manuscript has been revised by the American Journal Experts editing organization.

References

1. Ethier C, Oby ER, Bauman MJ, Miller LE. Restoration of grasp following paralysis through brain-controlled stimulation of muscles. Nature. 2012; 485:368–371. [PubMed: 22522928]
2. Moritz CT, Perlmutter SI, Fetz EE. Direct control of paralysed muscles by cortical neurons. Nature. 2008; 456:639–U663. [PubMed: 18923392]
3. Fasano A, Daniele A, Albanese A. Treatment of motor and non-motor features of Parkinson's disease with deep brain stimulation. Lancet Neurol. 2012; 11:429–442. [PubMed: 22516078]
4. Shannon RV. Advances in auditory prostheses. Curr Opin Neurol. 2012; 25:61–66. [PubMed: 22157109]
5. Mathieson K, et al. Photovoltaic retinal prosthesis with high pixel density. Nat Photonics. 2012; 6:391–397. [PubMed: 23049619]
6. Zrenner E, et al. Subretinal electronic chips allow blind patients to read letters and combine them to words. P Roy Soc B-Biol Sci. 2011; 278:1489–1497.
7. Ahuja AK, et al. Blind subjects implanted with the Argus II retinal prosthesis are able to improve performance in a spatial-motor task. Brit J Ophthalmol. 2011; 95:539–543. [PubMed: 20881025]
8. Pastrana E. Optogenetics: controlling cell function with light. Nature Methods. 2010; 8:24–49.
9. Mattis J, et al. Principles for applying optogenetic tools derived from direct comparative analysis of microbial opsins. Nature Methods. 2012; 9:159–231. [PubMed: 22179551]
10. Wallace GG, Moulton SE, Clark GM. Electrode-Cellular Interface. Science. 2009; 324:185–186. [PubMed: 19359568]
11. Owens RM, Malliaras GG. Organic Electronics at the Interface with Biology. Mrs Bull. 2010; 35:449–456.
12. Moulton SE, Higgins MJ, Kapsa RMI, Wallace GG. Organic Bionics: A New Dimension in Neural Communications. Adv Funct Mater. 2012; 22:2003–2014.
13. Bystrenova E, et al. Neural networks grown on organic semiconductors. Adv Funct Mater. 2008; 18:1751–1756.
14. Bolin MH, et al. Nano-fiber scaffold electrodes based on PEDOT for cell stimulation. Sensor Actuat B-Chem. 2009; 142:451–456.
15. Abidian MR, Ludwig KA, Marzullo TC, Martin DC, Kipke DR. Interfacing Conducting Polymer Nanotubes with the Central Nervous System: Chronic Neural Recording using Poly (3,4-ethylenedioxythiophene) Nanotubes. Adv Mater. 2009; 21:3764–3770. [PubMed: 26345408]
16. Richardson-Burns SM, et al. Polymerization of the conducting polymer poly(3,4-ethylenedioxythiophene) (PEDOT) around living neural cells. Biomaterials. 2007; 28:1539–1552. [PubMed: 17169420]
17. Gerard M, Chaubey A, Malhotra BD. Application of conducting polymers to biosensors. Biosens Bioelectron. 2002; 17:345–359. [PubMed: 11888724]
18. Arshak K, Velusamy V, Korostynska O, Oliwa-Stasiak K, Adley C. Conducting Polymers and Their Applications to Biosensors: Emphasizing on Foodborne Pathogen Detection. Ieee Sens J. 2009; 9:1942–1951.

19. Simon DT, et al. Organic electronics for precise delivery of neurotransmitters to modulate mammalian sensory function. Nat Mater. 2009; 8:742–746. [PubMed: 19578335]
20. Richardson RT, et al. Polypyrrole-coated electrodes for the delivery of charge and neurotrophins to cochlear neurons. Biomaterials. 2009; 30:2614–2624. [PubMed: 19178943]
21. Wan AMD, Brooks DJ, Gumus A, Fischbach C, Malliaras GG. Electrical control of cell density gradients on a conducting polymer surface. Chem Commun. 2009:5278–5280.
22. Schmidt CE, Shastri VR, Vacanti JP, Langer R. Stimulation of neurite outgrowth using an electrically conducting polymer. P Natl Acad Sci USA. 1997; 94:8948–8953.
23. Svennersten K, Bolin MH, Jager EWH, Berggren M, Richter-Dahlfors A. Electrochemical modulation of epithelia formation using conducting polymers. Biomaterials. 2009; 30:6257–6264. [PubMed: 19695696]
24. Blau A, et al. Flexible, all-polymer microelectrode arrays for the capture of cardiac and neuronal signals. Biomaterials. 2011; 32:1778–1786. [PubMed: 21145588]
25. Antognazza MR, Ghezzi D, Musitelli D, Garbugli M, Lanzani G. A hybrid solid-liquid polymer photodiode for the bioenvironment. Appl Phys Lett. 2009; 94
26. Ghezzi D, et al. A hybrid bioorganic interface for neuronal photoactivation. Nature Communications. 2011; 2
27. Pappas TC, et al. Nanoscale engineering of a cellular interface with semiconductor nanoparticle films for photoelectric stimulation of neurons. Nano Lett. 2007; 7:513–519. [PubMed: 17298018]
28. Goda Y, Colicos MA. Photoconductive stimulation of neurons cultured on silicon wafers. Nat Protoc. 2006; 1:461–467. [PubMed: 17406269]
29. Kong L, Zepp RG. Production and consumption of reactive oxygen species by fullerenes. Environ Toxicol Chem. 2012; 31:136–143. [PubMed: 21994164]
30. Jacobson SG, Cideciyan AV. Treatment possibilities for retinitis pigmentosa. N Engl J Med. 2010; 363:1669–1671. [PubMed: 20961252]
31. MacLaren RE, et al. Retinal repair by transplantation of photoreceptor precursors. Nature. 2006; 444:203–207. [PubMed: 17093405]
32. Pearson RA, et al. Restoration of vision after transplantation of photoreceptors. Nature. 2012; 485:99–103. [PubMed: 22522934]
33. Koch S, et al. Gene therapy restores vision and delays degeneration in the CNGB1-/- mouse model of retinitis pigmentosa. Hum Mol Genet. 2012
34. Busskamp V, et al. Genetic Reactivation of Cone Photoreceptors Restores Visual Responses in Retinitis Pigmentosa. Science. 2010; 329:413–417. [PubMed: 20576849]
35. Bi AD, et al. Ectopic expression of a microbial-type rhodopsin restores visual responses in mice with photoreceptor degeneration. Neuron. 2006; 50:23–33. [PubMed: 16600853]
36. Zrenner E. ARTIFICIAL VISION Solar cells for the blind. Nat Photonics. 2012; 6:342–343.
37. Polosukhina A, et al. Photochemical restoration of visual responses in blind mice. Neuron. 2012; 75:271–353. [PubMed: 22841312]
38. Natoli R, et al. Gene and noncoding RNA regulation underlying photoreceptor protection: microarray study of dietary antioxidant saffron and photobiomodulation in rat retina. Molecular vision. 2010; 16:1801–1823. [PubMed: 20844572]
39. Valter K, et al. Time course of neurotrophic factor upregulation and retinal protection against light-induced damage after optic nerve section. Invest Ophth Vis Sci. 2005; 46:1748–1754.
40. Delori FC, Webb RH, Sliney DH. Maximum permissible exposures for ocular safety (ANSI 2000), with emphasis on ophthalmic devices. J Opt Soc Am A. 2007; 24:1250–1265.
41. Sliney D. Exposure geometry and spectral environment determine photobiological effects on the human eye. Photochemistry and photobiology. 2005; 81:483–489. [PubMed: 15755194]
42. Butterwick, A., et al. Ophthalmic Technologies XVII. Stuck, BE., et al., editors. (SPIE Proceedings)

Europe PMC Funders Author Manuscripts

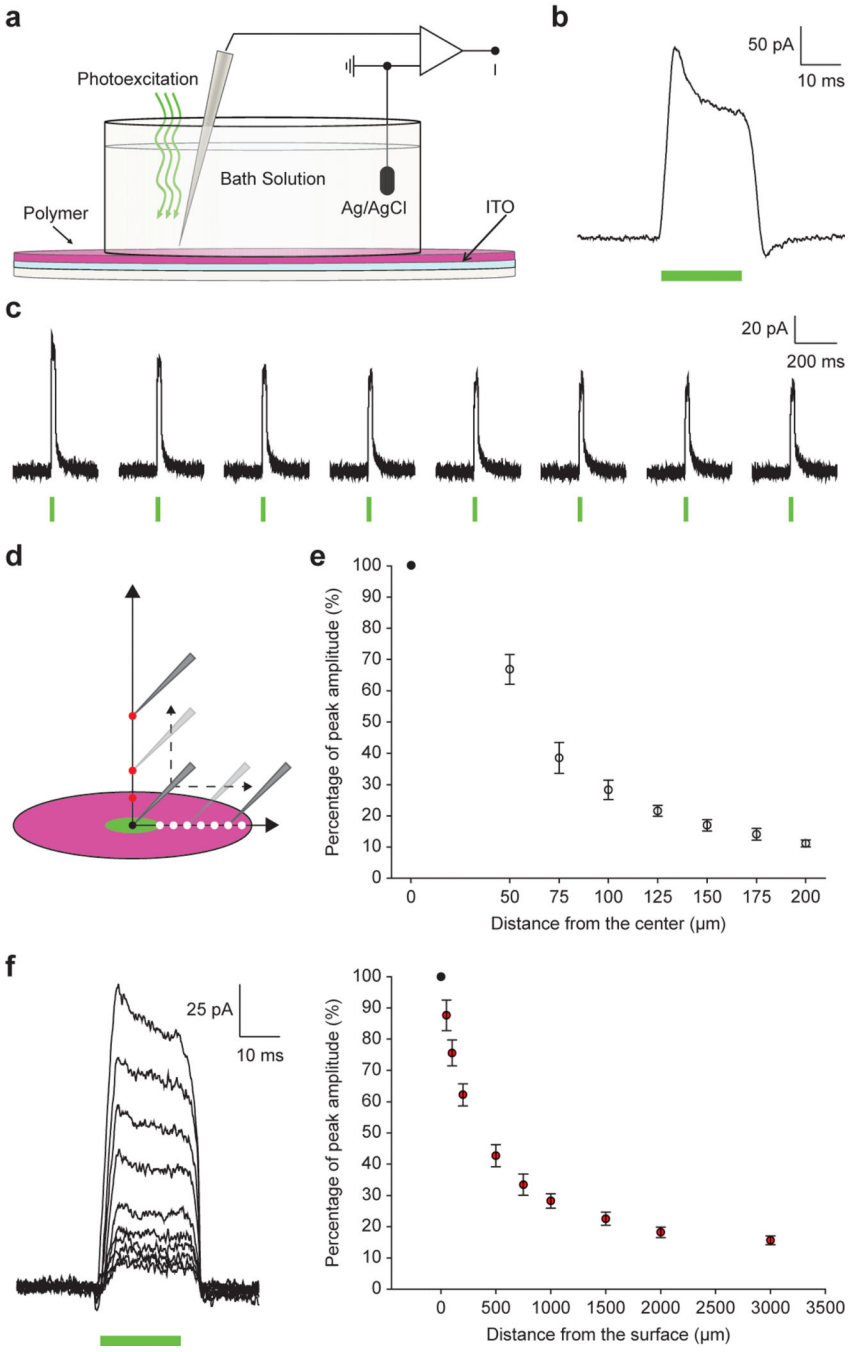

Figure 1. Characterisation of the photo-stimulus generated by the polymeric interface

(**a**) Schematic representation of the stimulation and recording paradigm. A patch-clamp amplifier was used to detect photo-currents generated upon light stimulation through a patch pipette positioned in close proximity (<5 μm) to the P3HT surface. (**b**) Photo-current detected in voltage-clamp mode upon light illumination (20 ms, 15 mW/mm^2; green bar). The trace represents an average of 5 consecutive sweeps. (**c**) Photo-currents generated upon repetitive light pulses (20 ms, 15 mW/mm^2; green bars) at a repetition rate of 2 Hz. A substantial preservation of the photo-current during the light pulse train was observed. (**d**)

Distribution of the photo-current along the P3HT surface and at increasing distances from the polymer surface. The green circle represents the light spot (100 μm, 20 ms, 15 mW/mm^2), whereas the white and red dots represent the points at which the patch pipette was sequentially positioned. The black dot represents the starting position. (**e**) The mean (± s.e.m.) photo-current along the P3HT surface, normalised to the amplitude of the first response, is shown as a function of distance from the spot centre (n = 6). (**f**) Photo-current detected in voltage-clamp mode upon light illumination at increasing distances from the polymer surface. The right panel shows the mean (± s.e.m.) photo-current intensity, normalised with respect to the amplitude of the first response, as a function of distance from the polymer surface (n = 6).

Europe PMC Funders Author Manuscripts

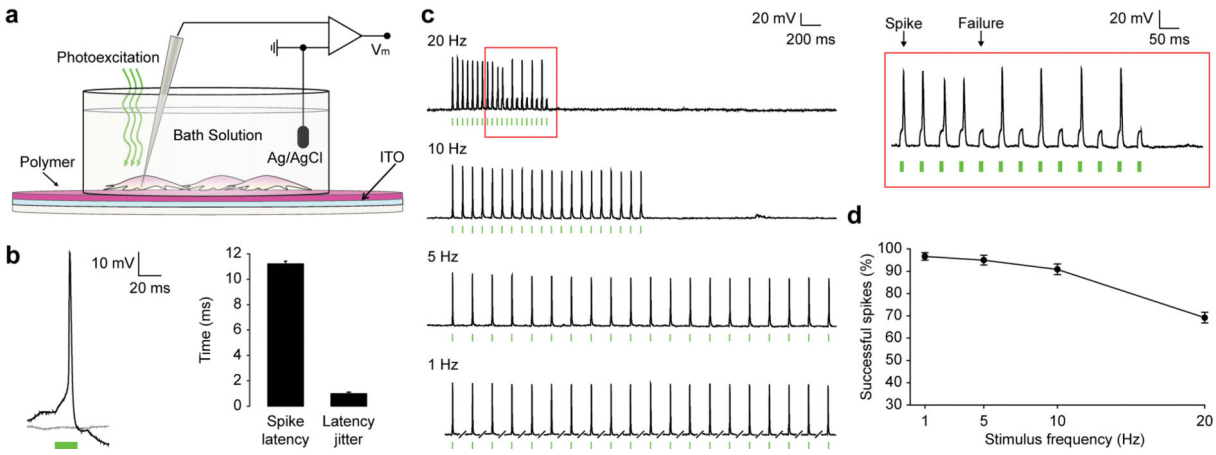

Figure 2. Photovoltaic excitation of neurons mediated by a P3HT active layer

(**a**) Schematic representation of the stimulation and recording paradigm. Neuronal responses to light illumination (20 ms, 15 mW/mm^2) were detected by patch clamp in current-clamp mode. (**b**) Activation by a light pulse (green bar) of a representative neuron cultured on a P3HT-coated Glass:ITO substrate (black) with respect to a neuron cultured on a control Glass:ITO coverslip (grey). The right plot shows the mean (± s.e.m.) latency to the spike peak with respect to light onset and latency jitter calculated as the standard deviation of spike latencies measured across all recorded neurons (n = 21). (**c**) Neuronal activation at various frequencies with a train of 20 stimuli (indicated by the green bars). The inset (red square) shows the spike or failure responses to the 20 Hz stimulation. (**d**) The percentage of successful spikes in the train of 20 pulses was computed over all recorded neurons and reported as a function of the stimulation frequency (n = 12, means ± s.e.m.).

Europe PMC Funders Author Manuscripts

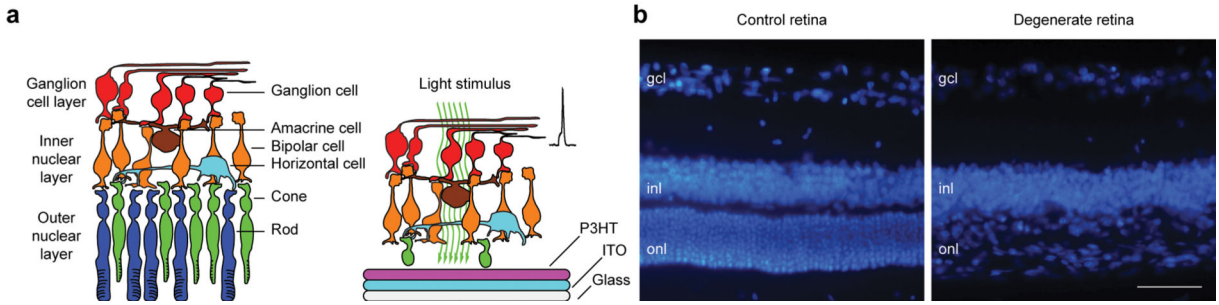

Figure 3. The photoreceptor layer is replaced in the degenerate retina by the organic polymer

(**a**) Schematic illustrations of the retinal structure (left) and the stimulation/recording interface for degenerate retinas (right). (**b**) Confocal images of latero-dorsal control (left) and degenerate (right) retinal sections labelled with the nuclear stain bisbenzimide (gcl: ganglion cell layer; inl: inner nuclear layer; onl: outer nuclear layer). Scale bar, 50 μm.

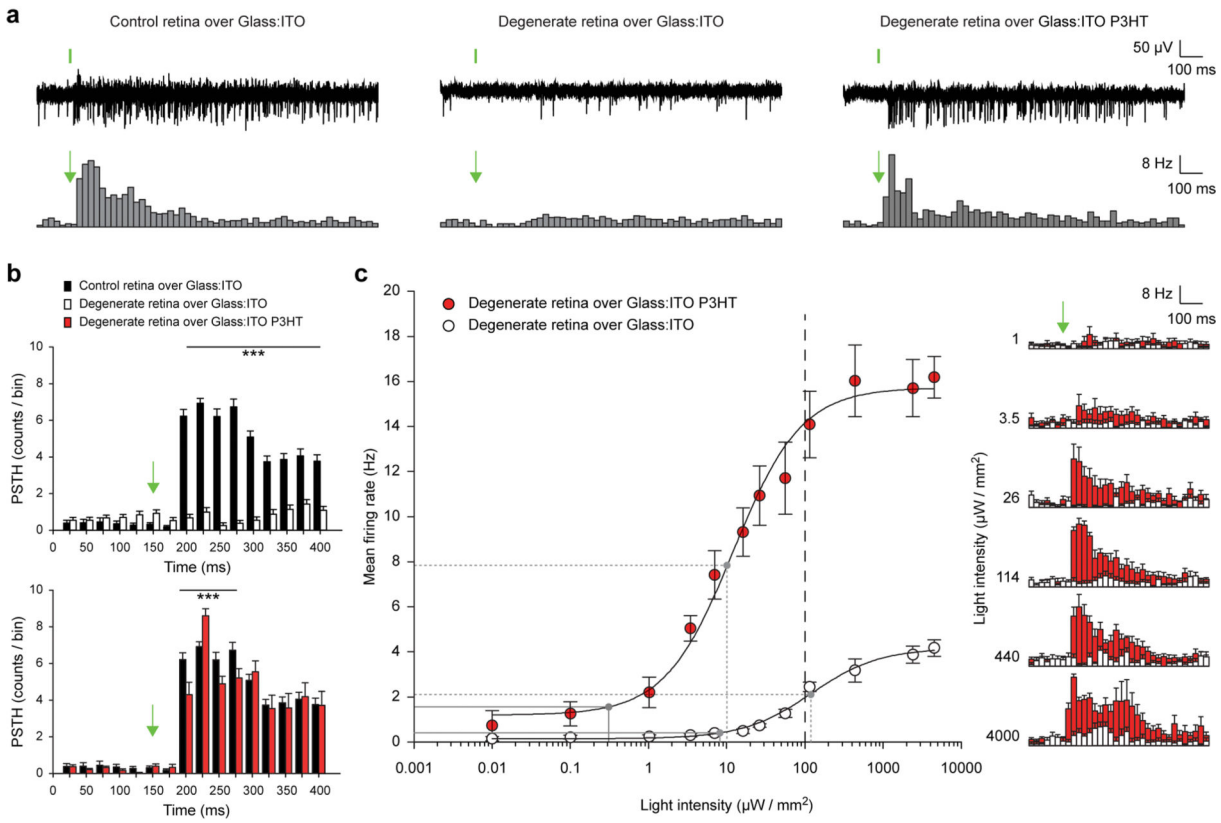

Figure 4. The P3HT layer restores responses in blind retinas

(**a**) Top panels show MUAs recorded upon light stimulation (10 ms, 4 mW/mm^2) of a control retina over a Glass:ITO substrate (left), a degenerate retina over a Glass:ITO substrate (middle) and a degenerate retina over a P3HT-coated Glass:ITO substrate (right). The bottom panels show normalised post-stimulus time histograms (PSTHs, bin: 25 ms) computed based on all sweeps recorded in single retinas (10 ms, 4 mW/mm^2) for the three experimental conditions. Green bars/arrows represent the light stimulus. (**b**) Comparison of mean (± s.e.m.) PSTHs (bin: 25 ms) obtained from control retinas on Glass:ITO (black bars, n = 5), degenerate retinas on Glass:ITO (open bars, n = 10) and degenerate retinas on P3HT-coated Glass:ITO (red bars, n = 10) in response to light illumination (10 ms, 4 mW/mm^2; green arrow). Significantly different bins are indicated (Student's t-test, P < 0.001). (**c**) Dose-response analysis of the mean (± s.e.m.) firing rate versus light intensity performed in degenerate retinas over P3HT-coated Glass:ITO (red dots, n = 6) or Glass:ITO alone (open dots, n = 6). Mean firing rates were calculated in a window of 250 ms after the light pulse. The dashed line represents the computed maximum permissible radiant power for a chronic exposure (see Methods). Dose-response curves were fitted using a sigmoidal dose-response model. Solid grey lines represent the response threshold (10% of the maximal response), and dotted grey lines represent the average ED_{50} calculated from the fitting procedure (12.11 and 120.78 µW/mm^2, respectively). On the right, representative PSTHs (bin: 25 ms, means ± s.e.m.) obtained in the presence (red) or absence (grey) of P3HT are shown. The green arrow represents the light stimulus.

Europe PMC Funders Author Manuscripts